JOURNAL OF MODERN OPTICS, 1993, VOL. 40, NO. 1, 23–32

Letter

Spatial grid symmetries and reduced models in the simulation of beam counterpropagation in a nonlinear medium

G. S. McDONALD† and W. J. FIRTH

Department of Physics and Applied Physics,
John Anderson Building, University of Strathclyde,
107 Rottenrow, Glasgow G4 0NG, Scotland

(*Received 13 October 1992 and accepted 25 October 1992*)

Abstract. In the context of the nonlinear interaction of counterpropagating light beams, we demonstrate the unrealistic symmetries that arise in the simulation of spontaneous pattern formation when using square computational grids. We have formulated a generalization of the split-step Fourier method which allows for non-orthogonal spatial grids. Implementation is shown to be simple and to entail negligible computational overheads. Results for two-dimensional Gaussian and extended cosine-bell input beam profiles are presented.

1. Introduction

In the modelling of nonlinear propagation of laser beams it has been common to analyse the electromagnetic field as simply planar thus removing any effects involving coordinates transverse to the direction of propagation. Consideration of transverse effects is bringing nonlinear optics much closer to real systems and also into the wider arena of space–time complexity [1–3]. To understand experimental configurations in which many physical processes take place, one has first to consider each component and its contribution to the whole. Here we focus on the basic configuration of just two beams of light which are counterpropagating in a passive nonlinear medium. Nonlinearity arises through the simple Kerr effect that reduces the model equations to a bare minimum in which significant spatiotemporal effects may arise. We concentrate on aspects of the numerical simulation of the problem and, in particular, present a reformulation of the standard split-step Fourier method which removes the symmetry constraints that are implicit in the use of orthogonal computational grids [4]. We also consider an approximation to Gaussian beam input which can reduce the otherwise enormous computational requirements of the problem while still retaining finite beam effects.

2. The model

The system under consideration consists of a slab, length L, of self-focusing material that is irradiated from each end by laser beams. The medium is assumed perfectly antireflection coated so that cavity effects do not occur. Diffraction and

† Present address: Optique Non-Linéaire Théorique, Université Libre de Bruxelles, Campus Plaine CP 231, 1050 Bruxelles, Belgium.

nonlinearity in the same medium leads to the consideration of a pair of coupled nonlinear Schrödinger-type equations for the evolution of the forward and backward (scalar) electric fields—F and B respectively.

$$\frac{\partial F}{\partial z}+\frac{\partial F}{\partial t}=\mathrm{i}\frac{\sigma}{2}\nabla_\perp^2 F+\mathrm{i}4\sigma(|F|^2+2|B|^2)F, \tag{1}$$

$$-\frac{\partial B}{\partial z}+\frac{\partial B}{\partial t}=\mathrm{i}\frac{\sigma}{2}\nabla_\perp^2 B+\mathrm{i}4\sigma(|B|^2+2|F|^2)B. \tag{2}$$

The input beams are assumed real and, generally, have a Gaussian amplitude profile

$$F(x,y,z=0)=F_0\exp[-(x^2+y^2)], \tag{3}$$

$$B(x,y,z=L)=B_0\exp[-(x^2+y^2)]. \tag{4}$$

The scaling of equations (1, 2) implies that the fields have amplitude units, as opposed to those of a nonlinear phase shift [5, 6]. We set $L=1$ and thus leave a single parameter, σ, which scales inversely with the (beam) Fresnel number. Numerical solution of (1)–(4) is performed using a split-step Fourier method modified to account for the simultaneous counterpropagation of the light fields [6–8]. Integration is performed along the characteristics and discretization in the resulting variables leads to an effective decomposition of the medium into a series of thin Kerr slices that partition regions of free space. In these empty regions diffraction may convert the nonlinear Kerr phase shift into an amplitude modulation [7]. Although analytic work has already been performed on this system [5, 6], a thorough exploration of the parameter spaces through numerical simulation is necessary to investigate the fully developed nonlinear dynamics. Even with only one transverse dimension, parameter sweeps can demand supercomputing resources. Any approximations which can reduce the computational load for simulations with *two* transverse dimensions have to be fully exploited.

The experiments of Grynberg *et al.* [9] revealed that a stationary hexagonal pattern of spots may arise in the far-field output of such a simple configuration. Their medium consisted of sodium vapour and cannot be fully described by the Kerr effect alone. It has been found, however, that such simple models of nonlinearity may indeed allow study of the essential features of pattern formation and, in particular, the spontaneous occurrence of hexagons on the output beams, a tendency which may be generic for third-order nonlinear systems [4, 10, 11]. The analysis of the problem in two transverse dimensions may be reduced to consideration of a set of interacting rolls [12, 13]. Each roll is essentially one dimensional in nature and can thus be orientated at any angle in the transverse plane. For a hexagonal pattern three equal amplitude rolls are required forming angles of $\pi/3$ to each other.

3. Spatial grid symmetries

For simulations with Gaussian beam input profile, we use a cartesian spatial grid with a minimum sampling density of 128×128. Results are checked using denser grids of up to 512×512 spatial points. Figure 1 (*a*) shows the stationary pattern that has developed on one of the output beams after a period of 150 medium transit times. While there are some small regions where a close-packed pattern is evident, the overall pattern has square symmetry. In figure 1 (*b*) we show an equivalent

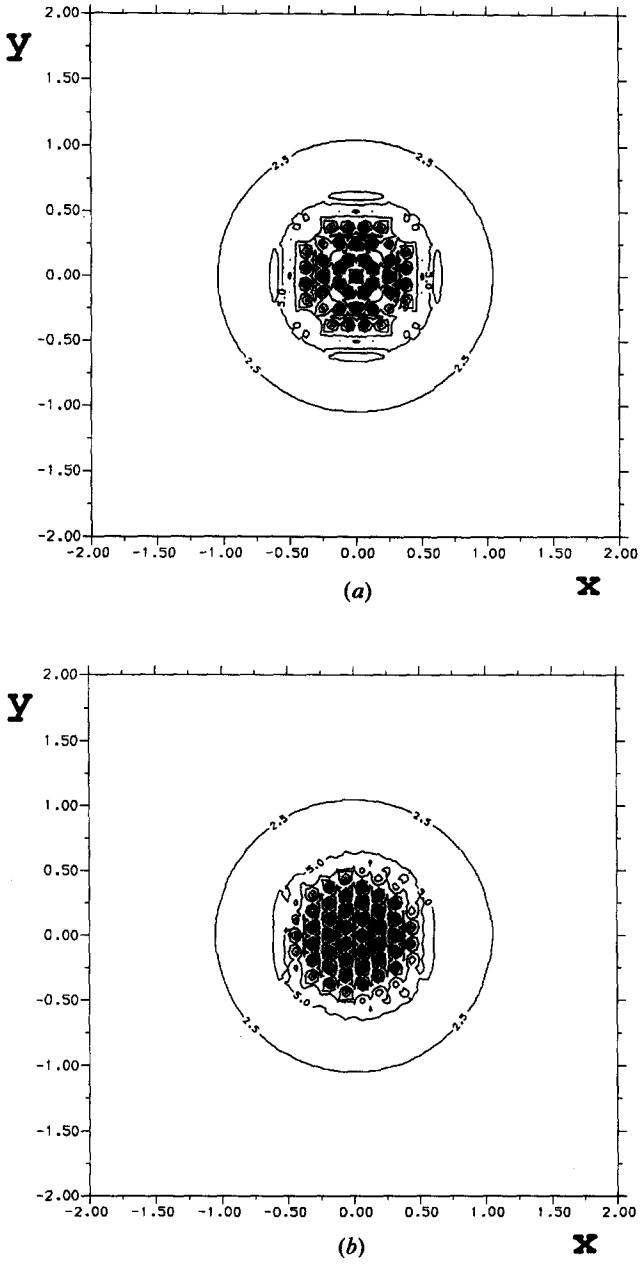

Figure 1. Spontaneous spatial patterns in the transverse plane of the output beam (Gaussian beam input, $F_0 = B_0 = 7{\cdot}5$, $\sigma = 0{\cdot}0025$). (*a*) Fourfold symmetries are imposed by the use of a square computational grid. (*b*) Inclusion of a small amount of noise on the input beams allows the system to select a hexagonal pattern of spatial filaments.

simulation but, in this case, a small amount of white noise (having amplitude 10^{-6}) has been included in the input fields [4]. This noise is sufficient to break the grid-imposed symmetry and permit the system to select the preferred pattern—a hexagonal array of spatial filaments.

There is always a finite amount of noise in any simulation and it is only when the level of this noise crosses some threshold that the symmetry imposed on the solution may be broken. Inclusion of a large amount of noise can, in some cases, induce numerical instabilities and result in unphysical dynamical effects. Further complication arises since the required level of any symmetry-breaking seed depends on the growth rate of the instability being constrained. Thus the use of noise to break imposed symmetries is not an entirely satisfactory situation. To resolve this we have solved system (1–4) by discretization of the solution on a non-orthogonal spatial grid. Defining a new transverse basis $(\mathbf{a}_1, \mathbf{a}_2)$ and coordinates with respect to this basis (x_1, x_2) one can write for any point, r, in the plane

$$r = x_1\mathbf{a}_1 + x_2\mathbf{a}_2. \tag{5}$$

The Kerr effect is spatially local and thus independent of the basis used. However, diffraction is a transverse coupling and the effect of this operator in the Fourier transform plane has to be re-evaluated for implementation of the split-step Fourier method. To do this we define projection vectors $(\mathbf{b}_1, \mathbf{b}_2)$, such that $\mathbf{b}_i \cdot \mathbf{a}_j = \delta_{ij}$ and consider the action of the Laplacian on an arbitrary scalar function $V(x_1, x_2)$. Defining the Fourier transform of this function, $\tilde{V}(K_1, K_2)$, through

$$V(x_1, x_2) = \int\int \exp\left[\mathrm{i}(K_1x_1 + K_2x_2)\right] \tilde{V}(K_1, K_2)\, \mathrm{d}K_1\, \mathrm{d}K_2, \tag{6}$$

then it can be shown that the operation $\nabla_\perp^2 V(x_1, x_2)$ is equivalent to

$$\int\int -\left[\mathbf{b}_1 \cdot \mathbf{b}_1 K_1^2 + \mathbf{b}_2 \cdot \mathbf{b}_2 K_2^2 + 2\mathbf{b}_1 \cdot \mathbf{b}_2 K_1 K_2\right] \exp\left[\mathrm{i}(K_1x_1 + K_2x_2)\right] \tilde{V}(K_1, K_2)\, \mathrm{d}K_1\, \mathrm{d}K_2. \tag{7}$$

From (7) it is clear that $(\mathbf{b}_1, \mathbf{b}_2)$ is the new basis in Fourier space so that at any point, $\mathbf{K}$, in the transform plane

$$\mathbf{K} = K_1\mathbf{b}_1 + K_1\mathbf{b}_2. \tag{8}$$

To explicitly demonstrate the numerical scheme we now choose a particular non-orthogonal space grid whose unit vectors form an angle of $\pi/3$. Since a hexagonal pattern may be constructed using equilateral triangles as building blocks, we are thus essentially considering a hexagonal grid. More specifically, we may choose $\mathbf{a}_1 = (1, 0)$ and $\mathbf{a}_2 = (\frac{1}{2}, \frac{\sqrt{3}}{2})$ which implies that $\mathbf{b}_1 \cdot \mathbf{b}_1 = \frac{4}{3}$, $\mathbf{b}_2 \cdot \mathbf{b}_2 = \frac{4}{3}$ and $\mathbf{b}_1 \cdot \mathbf{b}_2 = -\frac{2}{3}$. In the symmetrized split-step solution of (1, 2) the (forward field) solution is advanced

$$F(x, y, z + \Delta z) = \exp\left(\mathrm{i}\frac{\sigma}{2}\frac{\Delta z}{2}\nabla_\perp^2\right) \exp\left[\mathrm{i}\Delta z(|F|^2 + 2|B|^2)\right] \exp\left(\mathrm{i}\frac{\sigma}{2}\frac{\Delta z}{2}\nabla_\perp^2\right) F(x, y, z), \tag{9}$$

and the diffraction operator becomes the following multiplication in the transform plane

$$\exp\left[-\mathrm{i}\frac{\sigma}{2}\frac{\Delta z}{2}\frac{4}{3}(K_1^2 + K_2^2 - K_1K_2)\right] \tilde{F}(K_1, K_2, z). \tag{10}$$

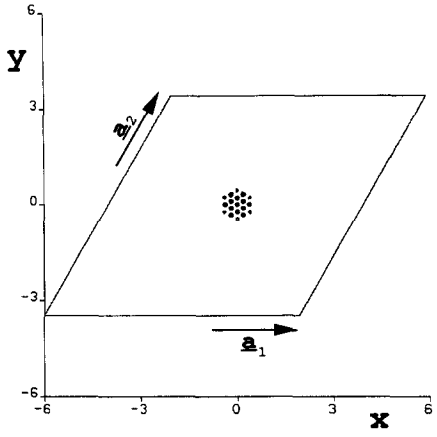

Figure 2. Array of sharp spatial filaments at the centre of the output beam when spatial discretization is on a hexagonal grid. The whole computational grid is shown ($\Phi = \pi/3$, other parameters are as in figure 1).

In the general case of a grid whose basis vectors form an angle of Φ then (10) becomes

$$\exp\left\{-\mathrm{i}\frac{\sigma}{2}\frac{\Delta z}{2}\frac{1}{\sin^2\Phi}[K_1^2+K_2^2-2\cos(\Phi)K_1K_2]\right\}\tilde{F}(K_1,K_2,z). \tag{11}$$

In figure 2 we show the results after performing the same simulation as figure 1 (*b*) but now with calculations made on our hexagonal grid. Here the solution has converged to the hexagonal pattern without the addition of noise.

4. Transverse and longitudinal boundary conditions

We have simulated a variety of different longitudinal boundary conditions in addition to incident Gaussian beams. Plane wave excitation is the most simple and permits the usage of relatively few transverse sampling points (64×64). Above the threshold, the plane wave solution is unstable to formation of spatial patterns, but to allow such patterns to form (consuming only a reasonable amount of computer time) one needs to perturb or seed the initial fields in the medium. Given that noise may introduce unwanted effects and that the solution depends on the amount of noise added, one may adopt trial solutions for the fields along the medium. This approach is satisfactory only if one knows, or can prove, that such a solution, if stable, is not merely a local minimum in some potential and that it is stable to perturbations of an arbitrary transverse structure. Unfortunately, the most suitable candidate for this arbitrary perturbation is noise itself. Planar pumping may also impose unrealistic spatial boundaries at the edges of the computational grid. The split-step Fourier method uses fast Fourier transforms which enforces periodicity in both the x and y directions. One thus models a zone of an implicitly infinite periodic spatial pattern. This symmetry forces each zone to mirror its neighbours restraining the interaction between zones and, by consequence, the resulting patterns that may form.

It is important to consider what effect that the size of the computational box may have on the resultant pattern and if any grid resonances may arise. A sensible approach to minimize the effects of periodicity is to define the box length, l_b, to be an integer multiple, n, of the most unstable spatial wavelength, λ_u. Generally, we find

that the spatial orientation of the pattern may change and that there may be a longer time needed for convergence of the solution in simulations where l_b is chosen to deviate from $n\lambda_u$. Unlike simulations in only one transverse dimension, $l_b = n\lambda_u$ is not the only criterion for pattern convergence. This can be simply envisaged through considerations of attempting to squeeze a hexagon pattern into a square box.

A further refinement to the planar pumping scheme is to seed a trial solution in only a small region at the centre of the spatial grid. In this case we typically multiply the solution seed by a two dimensional extended cosine-bell (2DEC) spatial envelope. We have found that using this envelope (defined in figure 3) allows the system more freedom to select a preferred pattern. The envelope seeds a range of spatial frequencies while, in the initial stages of the simulation, the effect of the spatial boundary conditions is greatly reduced. Classic defect structures, such as penta–hepta pairs, often appear as transient structures when nucleating patterns attempt to interlock at the edges of the computational grid. The planar pumping approximation constitutes an essential tool for the study of pattern formation in laser optics but one must eventually progress to finite beam effects and the massive computational overhead which this usually entails.

We have found that the implementation of 2DEC input profiles (figure 3) may produce results that are qualitatively the same as those for Gaussian beam input. In both cases the structure of the input field implies a finite band of injected spatial frequencies which can seed transverse instabilities and allow them to become quickly established. The advantage is that the 2DEC input approximation can lead to major computational savings. First, it allows maintenance of a well-defined and smooth central beam region where regular patterns may form—the precisely known input value of the central region lending itself to straightforward comparison with plane wave analyses. Spatial variation of the pump beams can imply that the output profile will be composed of a mixture of patterns. A large region of uniform input allows one to verify whether there is a correspondence between, say, local incident intensity and a specific output pattern. To obtain an equivalent region at the centre of a Gaussian beam would require a very wide beam and a similarly large numerical grid with the associated leaps in required computer time and memory usage for any simulation.

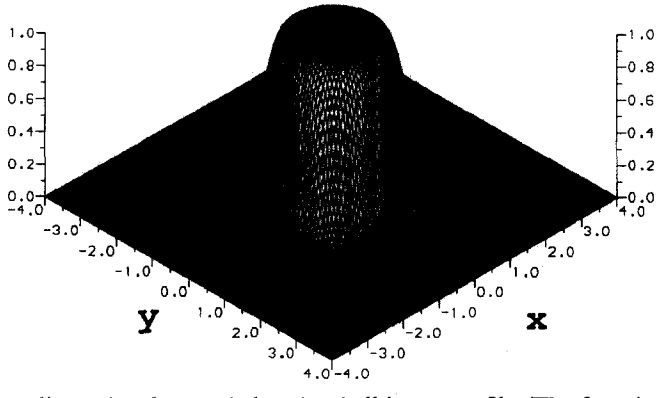

Figure 3. Two-dimensional extended cosine-bell input profile. The function defines a flat circular region at the centre of the grid ($F(z=0)=B(z=L)=f_0$ for $r=(x^2+y^2)^{1/2} < T_{max}/4$) and a background of zero field ($F(z=0)=B(z=L)=0$ for $r > T_{max}/2$). The two flat sections are joined smoothly by a cosine function.

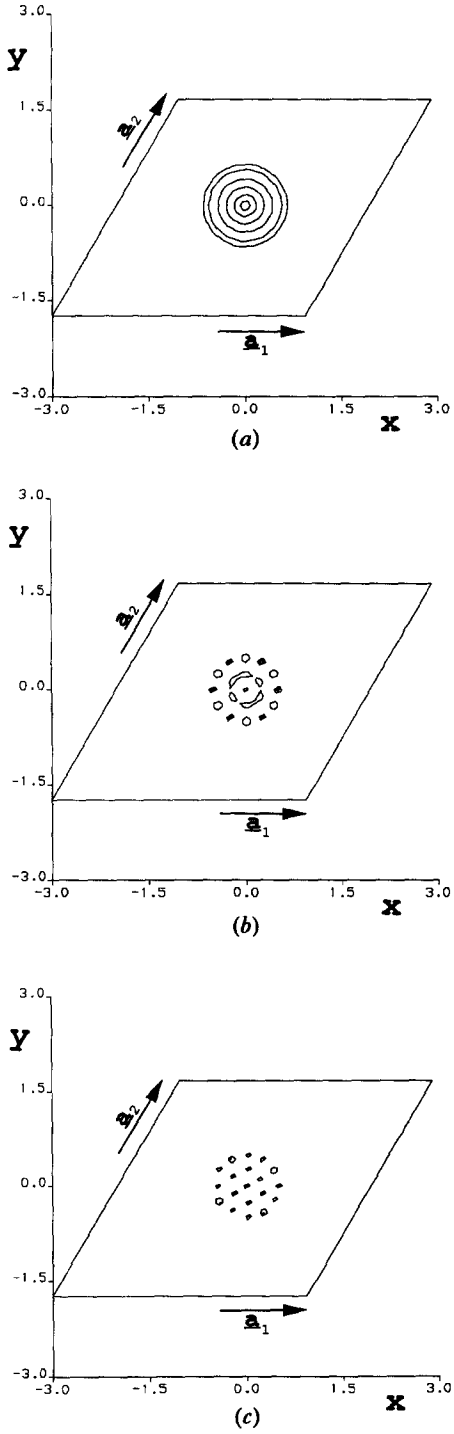

Figure 4. Simulation on a non-orthogonal spatial grid and using two-dimensional extended cosine-bell (2DEC) pump profiles. (*a*) Transient rings form on the output beams ($t=20$). (*b*) Modulational instability breaks up the rings ($t=30$). (*c*) Spatial filaments arrange themselves into a hexagonal pattern ($t=40$). Parameters are $\Phi=\pi/3, f_0=3{\cdot}43$, $\sigma=0{\cdot}01$, and t is in units of cavity transit times.

Second, to maintain accuracy of the numerical integration, one requires the electric field to be sufficiently negligible over half of the computation grid. This favours the use of the 2DEC input approximation since, instead of a slow exponential profile decay, the input level may be defined to rapidly approach and attain zero field near to the region of pattern formation.

Results from a simulation with 2DEC pump field and performed on a non-orthogonal grid are shown in figure 4. Even though only 64×64 spatial grid points have been used, this simulation demonstrates the sequence which gives rise to spontaneous hexagon formation on wide Gaussian beams. There has been no artificial noise added here. Instead, the rapid spatial variation of the input profiles seeds an instability that grows and develops in a relatively short integration period. In figure 4 (*a*) the output beam has a well-established ring structure. Rings occur because the central flat region of the input is above the threshold for modulational instability and since, initially, there is no preferred transverse direction for the most unstable spatial wave-vector. Subsequent developments, figure 4 (*b*), show a second

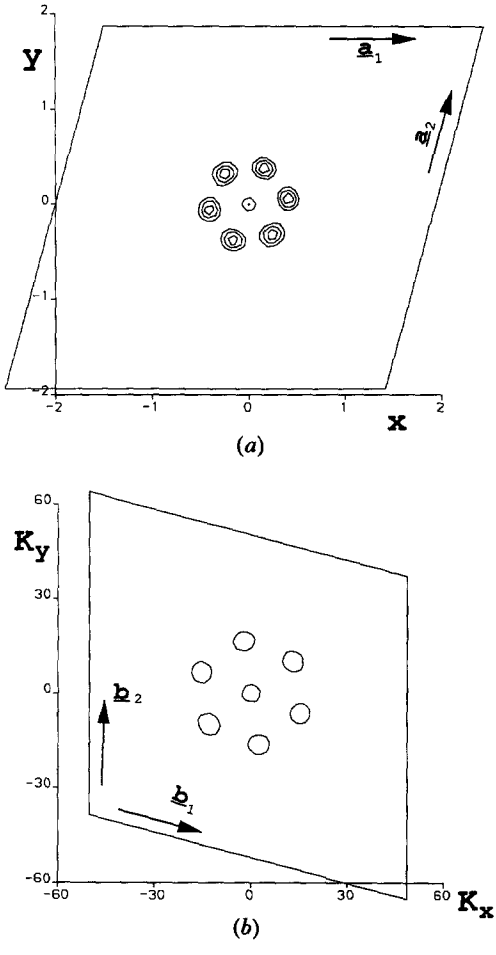

Figure 5. Output patterns for 2DEC input calculated on a spatial grid whose basis vectors form an angle of 75° ($f_0 = 2{\cdot}127$, $\sigma = 0{\cdot}026$, $t = 20$). (*a*) Wide spatial filaments form a hexagon. (*b*) Positions of the corresponding peaks in the transform plane.

modulational instability—this time along the smooth ridges of the rings which leads to the break-up of the output pattern into spots. The final part of figure 4, at only $t=40$, shows that the spots arrange themselves into a uniform hexagonal pattern.

Our results would be incomplete if non-hexagonal grids were not to be considered. In figure 5 we show the output pattern for a grid angle $\Phi=75°$ and, again, 2DEC input profiles. In figure 5 (*a*) a hexagonal pattern of wide spatial filaments can be seen while in figure 5 (*b*) we show the Fourier transform (far-field) image. Recall that $\mathbf{b}_i \cdot \mathbf{a}_j = \delta_{ij}$ and thus the angle of the transform grid is $180° - \Phi$.

Since spontaneous spatial patterns are only expected above a certain input level, a natural spatial boundary effect will occur at some distance from beam centre for both Gaussian and 2DEC pump fields. The role of this boundary and its effect on pattern nucleation is still not properly understood. Other subjects of interest are the conditions for the formation of any defect points or lines and their relation to the neighbouring or host pattern. Such studies require large arrays of spatial filaments and, while experimentally this may not pose great difficulties, the computational requirements could be prohibitive. The implementation of 2DEC input, or some equivalent approximation such as super-Gaussian profile, may allow computer simulation to address such questions in the near future.

5. Conclusions

We have demonstrated that caution is necessary in the numerical simulation of spatial pattern formation. The use of a square computational grid may lead to patterns constrained by the imposed symmetry. Addition of a small amount of noise to the solution may break the symmetry constraint, but, at the same time, introduce further dependencies and, sometimes, unwanted effects. Input profile of cylindrical symmetry is not sufficient to break the fourfold grid symmetry as we have shown in the case of input Gaussian beams. We have formulated the use of non-orthogonal grids in the split-step Fourier method. Its implementation is trivial and does not impose any appreciable computational overhead. At the start of any simulation one calculates, and stores, a modified array which is used in place of the standard (diffraction operator) array. We have also discussed pattern formation under planar pumping and presented results for a two dimensional extended cosine-bell approximation to the Gaussian pump field.

The central theme of this paper has been the valid reduction of a massively intense computational problem in pattern formation, which typically requires many cpu hours on a Cray supercomputer for its complete solution. We have presented a reduced model which parametrizes all the complexity of the full problem but which may be solved on a dedicated workstation. Indeed, most of the basic phenomena and discussions are essentially independent of the model equations. The considerations made here may well be applicable to a wide range of physical problems.

Acknowledgments

The authors take great pleasure in the acknowledgement of many enlightening discussions with G. D'Alessandro, C. Penman, E. M. Wright, J. V. Moloney, R. Indik, R. Chang, J. B. Geddes and C. Pare. This work is supported in part by SERC grants GR/F 49811, GR/F 76502 and GR/G 12665 and in part through a Twinning project of the European Communities.

References

[1] BISHOP, A. R., GRUNER, G., and NICOLAENKO, B., editors, 1986, *Physica* D, **23,** 1.
[2] DOOLEN, G., ECKE, R., HOLME, D., and STEINBERG, V., editors, 1989, *Physica* D, **37,** 1.
[3] ABRAHAM, N. B., and FIRTH, W. J., 1990, *J. opt. Soc. Am.* B, **7,** 951.
[4] CHANG, R., FIRTH, W. J., INDIK, R., MOLONEY, J. V., and WRIGHT, E. M., 1992, *Optics Commun.*, **88,** 167.
[5] FIRTH, W. J., and PARE, C., 1988, *Optics Lett.*, **13,** 1096.
[6] FIRTH, W. J., FITZGERALD, A., and PARE, C., 1990, *J. opt. Soc. Am.* B, **7,** 1087.
[7] FIRTH, W. J., PENMAN, C., and PARE, C., 1990, *Optics Commun.*, **75,** 136.
[8] HARDIN, R. H., and TAPPERT, F. D., 1973, *SIAM Rev.*, **15,** 423.
[9] GRYNBERG, G., LEBIHAN, E., VERKERK, P., SIMONEAU, P., LEITE, J. J. R., BLOCH, D., LE BOITEAUX, S., and DUCLOY, M., 1988, *Optics Commun.*, **66,** 321.
[10] D'ALESSANDRO, G., and FIRTH, W. J., 1991, *Phys. Rev. Lett.*, **66,** 1597.
[11] D'ALESSANDRO, G., and FIRTH, W. J., 1992, *Phys. Rev.* A, **46,** 537.
[12] HAKEN, H., editor, 1984, *Chemical Oscillations, Waves and Turbulence*, Springer Series in Synergetics, Vol. 19 (Berlin: Springer-Verlag).
[13] CILIBERTO, S., COULLET, P., LEGA, J., PAMPALONI, E., and PEREZ-GARCIA, C., 1990, *Phys. Rev. Lett.*, **65,** 2370.